Local environment of nitrogen in a surface nitride: A low-energy electron diffraction study of Cr(100)-(1×1)N

Y. Joly, Y. Gauthier, and R. Baudoing
Laboratoire de Spectrométrie Physique, Université Joseph Fourier, Boîte Postale 87, 38402 Saint Martin d'Hères CEDEX, France
(Received 3 May 1989; revised manuscript received 28 July 1989)

We present a quantitative low-energy electron diffraction study of the surface nitride produced by nitrogen segregation to the surface of the (100) face of chromium. Emphasis is put on the local environment of N atoms, in reference to surfaces of bulk nitrides, this study being one step in a longer-term investigation of the role of vacancies at substoichiometric nitride and/or carbide surfaces. The nitrogen atoms are found to occupy symmetric fourfold hollow sites. The nitrogen atoms are 0.221±0.016 Å above the chromium first layer and have four metal neighbors in the top layer with a 2.045±0.002 Å bond length and a fifth metal neighbor in the second layer at a very similar distance, 2.015±0.018 Å. This environment is made possible by having a very large expansion (24.8%) of the topmost interlayer spacing of chromium and shows great similarities with the surface structures of : (i) surface nitrides like Ni(100)-$P4g$-(2×2)-N (which reconstructs with a large lateral displacement of the surface metal atoms), Fe(100)-c(2×2)-N (which does not reconstruct because the metal substrate is bcc like chromium, leaving room for the N atoms to set up the maximum coordination), and (ii) the surface of a bulk nitride $VN_{0.89}$(100) (as obtained from preliminary results).

I. INTRODUCTION

The electronic and crystallographic properties of chemisorbed small atoms such as nitrogen, oxygen, carbon, sulfur, etc., on the low-index faces of transition metals have been the subject of extensive experimental and theoretical investigations.[1,2] These studies have attempted to characterize the chemisorption site, the presence or not of reconstruction of the surface, the influence of the adsorbate on the relaxation of the topmost layers of the substrate,[3] and finally the local environment of the adsorbed atom to reach a general view and comprehension of these surface structures. Due to the small size of these adsorbates, many positions become possible: in particular, the occurrence of low-symmetry sites, where N is bound to two or three metallic atoms cannot *a priori* be excluded and need to be explored in any thorough analysis. However, adsorption at the high-symmetry fourfold site is the most common.

Nitrides and carbides are also a subject of great interest.[4–7] In particular, the bulk properties of high mechanical hardness and chemical stability are at the origin of many applications. The surface properties of these compounds have only begun to be studied,[8,9] particularly in view of the relatively large amount of vacancies in substoichiometric compounds.

Very often, nitrogen (or carbon) adsorbed on a metal comes to form a "surface nitride (or carbide)" and it is a matter of interest to make the link between these compounds with the surface of "bulk nitrides." In this context we present a low-energy electron diffraction (LEED) study of Cr(100)-(1×1)-N.

The paper is arranged as follows: Sec. II describes the experimental procedure, Sec. III is concerned with the LEED analysis itself, and Sec. IV presents a discussion of results. A comparison with similar surface compounds and with preliminary results obtained on the surface structure of $VN_{0.89}$(100) is given.

II. EXPERIMENT

The experiments were performed in a standard UHV system, equipped with a hemispherical display-type LEED diffractometer[10] having complete freedom for the incident and diffracted beam directions and with a high angular precision (<0.1°) and a high sensitivity. The optics, acting as a retarding field analyzer, are used for Auger electron spectroscopy (AES). Beam intensities are measured by means of a spot photometer, fixed on a two circle goniometer mounted above the hemispherical screen. Cancellation of magnetic fields is achieved by means of three big Helmholtz coils.

The chromium sample (bcc structure with a lattice parameter a=2.875 Å) was spark cut from a rod and oriented using x rays. Mechanical and electrochemical polishing produced a surface within 20′ of the true crystallographic (100) plane. This surface was then cleaned *in situ* by numerous cycles of argon bombardment (60 min, 10 mA, 500 eV) followed by annealing (30 min, 750 °C). As the main impurities (sulfur and oxygen) disappeared, nitrogen segregated to form a (1×1) overlayer, with a $P4m$ symmetry in the LEED pattern. AES revealed that a real nitride forms at the surface, and nitrogen segregated from the bulk was found to form a very stable and very reproducible structure.

LEED $I(V)$ curves were recorded at normal incidence and at two oblique incidence conditions $(\theta,\phi)=(10°,0°)$ and $(34°,45°)$. For $\phi=45°$, the incidence plane is parallel to the [011] direction. Although very good agreement was obtained for symmetrically equivalent beams, they

were averaged to produce optimized spectra. The final data set considered in the analysis contained 23 nonequivalent beams for a total energy range of about 3000 eV. The spectra recorded on a 1-eV grid were normalized to constant incident current, after background subtraction.

III. LEED ANALYSIS

A. Calculational aspects

1. LEED program

LEED intensity calculations were performed using a layer-by-layer program fitted with a layer doubling routine[11] for bulk planes. This code can handle several atoms in the unit mesh, allowing treatment of complex surface layers as well as small interlayer distances. The top layer containing Cr and N atoms was treated as a "thick mixed" layer using a spherical wave representation and a matrix inversion to deal with multiple scattering.

2. Optical potential

The energy-dependent inner potential $V_R(E)$ is calculated using a formalism proposed by Hedin and Lundqvist.[12] This model was checked experimentally in LEED for Cu(100), using threshold effects,[13] and for Ni(110) (Ref. 14) from LEED $I(V)$ analysis: the shape of this potential variation proved to be very similar in both metals, the only difference being essentially a small rigid shift ΔV_R. Consequently in the final step of the analysis (calculation of the metric distance) $V_R(E)$ is allowed to be shifted rigidly by a small amount ΔV_R to account for a slight difference between Cu, Ni, and Cr.

The absorptive potential, energy dependent as well, is given the value used in previous papers.[13–15] The Debye temperatures were fixed at 600 and 485 K for N and Cr, respectively. All these parameters were given the same value for bulk and surface layers.

3. Optimizing the structure

The intensities resulting from LEED calculations were compared to experimental data via five metric distances previously described in detail,[16] namely D_1, D_2, D_{2y}, D_4, and D_{4y}. These distances are numerical criteria used to measure the quality of the agreement between experimental and theoretical spectra similar to the reliability factor well known in x-ray analyses: the lowest the metric, the better the model. They proved very efficient in a number of studies of clean and covered metal and alloy surfaces.[3,13,15,17–21]

4. Muffin-tin radius

The phase shifts result from the superposition of atomic densities for N and Cr species, including four shells of neighbors; the phase shifts of surface metallic atoms were calculated according to their actual neighborhood. Convergence was ensured by using up to nine phase shifts at the highest energy. The radius of N atoms is known to span a wide range depending on the material, it was thus allowed to vary from 0.5 to 0.85 Å in the calculations. A consequence of this small size is that adsorption in the second and following layers cannot be excluded *a priori:* for instance, N adsorbs in underlayer sites at Ti(0001).[22]

5. Models under investigation

In this work many adsorption sites were thus tested, including fourfold top and hollow sites (over and underlayer), twofold bridge sites (over and underlayer). Moreover, N might adsorb above the substrate in low-symmetry sites of coordination 3, in contact with two surface Cr atoms and one second layer Cr atom, i.e., at intermediate positions between bridge and fourfold hollow sites, with a mirror symmetry (sites labeled MO in Fig. 1). In order to retain the fourfold symmetry of the LEED pattern, domain averaging was performed where necessary. While in the hcp structure of bulk Ti small atoms have room to adsorb anywhere, the interstitial sites in bulk bcc materials are very small so that nitrogen adsorption is not possible without very large expansions of interlayer distances. For example, bridge underlayer sites require spacings to be enlarged by about 40%, which seems unlikely in view of the energy necessary to move a layer by such large amounts. Nevertheless, owing to the strength of the nitride bond and to the possibility of underlayers, we considered, in addition to the adsorbate lo-

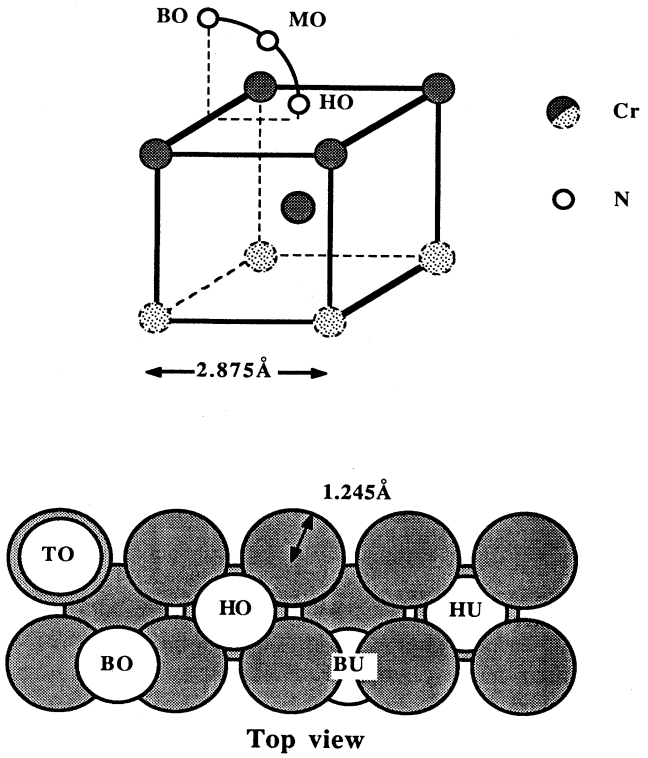

FIG. 1. Cr(100)-(1×1)N: bulk Cr structure and adsorption sites investigated in the present study: bridge overlayer (BO) and underlayer (BU), fourfold on top (TO), fourfold hollow overlayer (HO) and underlayer (HU), and mirror (MO) sites (see text).

cation, very large relaxations of the interlayer distance d_{12} (50% contraction up to 45% expansion) simultaneously with large variations of the adsorbate-substrate distance, d_{N1}.

B. Analysis

All the calculations were done on a 4-eV energy grid, which has been proven to be the optimum compromise between a very good stability of the metric distances against the energy step and the computing cost. The analysis was performed in two successive steps. First, the analysis was restricted to the normal incidence data set corresponding to the most symmetrical condition and hence to the smallest computing time. This eliminates a lot of adsorption sites and, for the very few probable ones, to locate a unique minimum close to the best values for each parameter on a coarse scale. Then we refine the parameters around the unique minimum by analyzing the full data base at the same time.

1. Normal incidence data

By these preliminary calculations we could discard unambiguously (Fig. 1) bridge (BO), on top (TO), underlayer hollow (HU), bridge underlayer (BU), and less usual sites (MO); indeed, all these models yield very large metric distances, typical of improbable sites: $D_1 \geq 30\%$ to be compared with the final value $D_1 \sim 11\%$ for the optimum model at normal incidence. It is of some importance to consider MO positions since for small adsorbates there has been a controversy about the possibility of adsorption in low-symmetry sites. For this site, the agreement improves continuously when going from the BO to the HO position.

Figures 2 and 3 compare theoretical spectra, calculated for various adsorption sites and various spacing values d_{12}, respectively, with the corresponding experimental data at normal incidence. The best solution corresponds to N adsorbed in the hollow site (HO), slightly above the substrate, and a large expansion of the interlayer spacing d_{12}.

A contour plot of the metric distance D_1 is illustrated in Fig. 4 for the fourfold hollow site (HO). The map is restricted to expanded interlayer spacings d_{12} for a wide range of adsorbate-substrate distances d_{N1}. Models with shortened spacings yield a bad agreement and correspond to a strong (unphysical) overlap of metallic and nitrogen

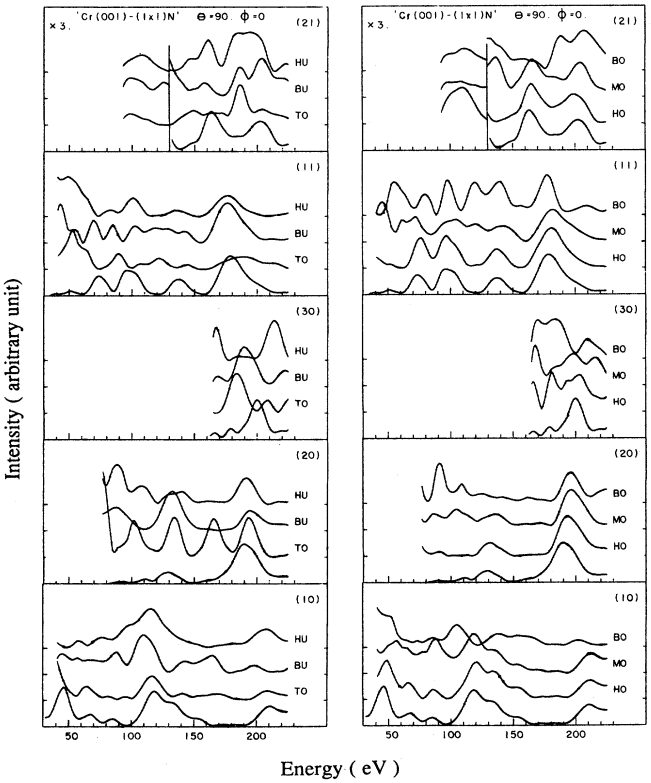

FIG. 2. Normal incidence $I(V)$ spectra for the best relaxations with nitrogen adsorbed in different sites. Calculation compared to experiment (bottom curve). See legend of Fig. 1 for the definition. The best agreement is obtained for the fourfold hollow site (HO).

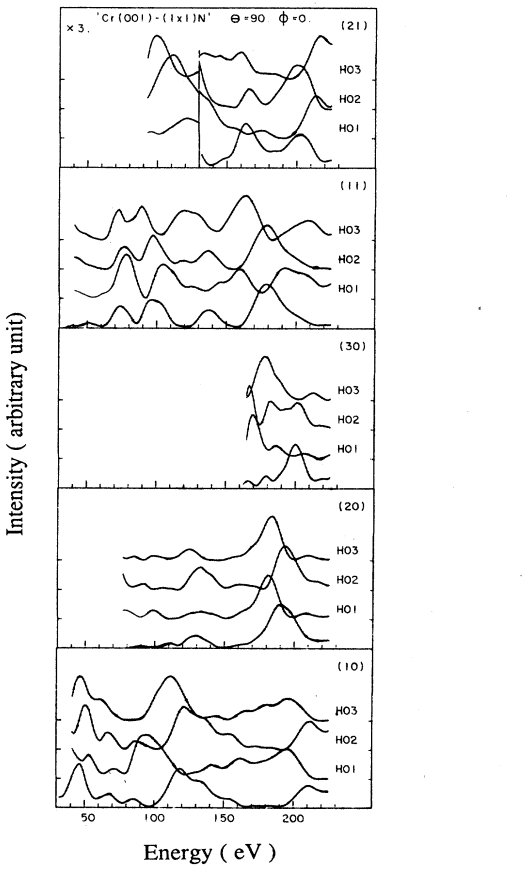

FIG. 3. Normal incidence $I(V)$ spectra for nitrogen adsorbed in the fourfold hollow site (HO) at three interlayer relaxation values for d_{12} corresponding to 5% (HO1), 25% (HO2), and 45% (HO3) relaxation, respectively, in comparison to experiment (bottom curve). These models are shown for the best distance d_{N1}.

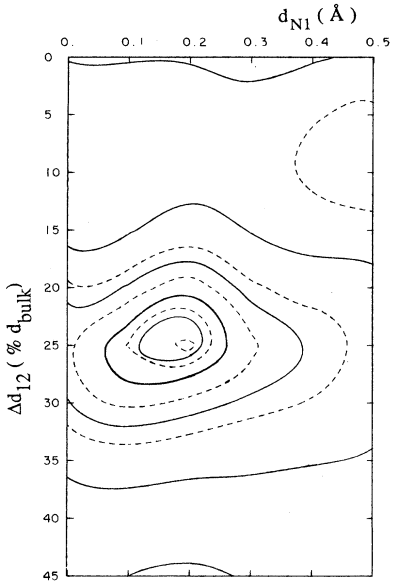

FIG. 4. Two-dimensional contour map of metric distance D_1 with N in the fourfold hollow site (HO), for normal incidence data analysis only. The contour levels are arranged according to the following law: $[d_{min}+(d_{max}-d_{min})2^n/100]$, where d_{min} and d_{max} represent, respectively, the minimum and maximum of the metric distance in the whole range of parameters. Note that only one sharp minimum appears.

atoms. For positive relaxations, the map shows a clear and unique minimum centered at about 25% relaxation (which is not common for bcc metals) and a vertical nitrogen-chromium distance d_{N1} of about 0.2 Å.

2. Complete data base

In the second step, calculations included the three incidence conditions $(\theta,\phi)=(0°,0°)$, $(10°,0°)$, and $(34°,45°)$, and were limited to the fourfold overlayer hollow site in order to refine the parameters d_{N1}, d_{12}, and d_{23}. Finally, owing to possible charge transfer between nitrogen and the metal, predicting the actual size of the adsorbate is not straightforward. Hence, in addition to the above-mentioned parameters, the nitrogen muffin-tin radius was optimized simultaneously. This was done as follows: using the structural parameters found from the normal incidence data set, we computed a new muffin-tin potential from the superposition of atoms placed at the correct distances and derived from them new phase shifts for the nitrogen and chromium atoms located in the top mixed layer. For nitrogen, the muffin-tin radius is then optimized simultaneously with the structural parameters.

C. Results

1. Level of agreement

The final agreement for the best structure is remarkable as evidenced by the very low value of the metric distances obtained for the whole set of data as well as the very small dispersion of the optimum values for the parameters given by the various metrics (see Table I). This is also confirmed by the visual inspection of spectra (Fig. 5): all features of experimental spectra are present in the theory and correctly described but for some limited structures, in the (30) beam at $\theta=0°$ for instance.

Table II provides more detailed information: for each data set, independently, we have listed the best parameters obtained as the average answer from the five metric distances together with the standard deviation. We emphasize that one should not regard this latter value as the ultimate uncertainty of LEED analysis but rather as an indication of the level of consistency in comparing this particular set of data with the LEED best model; each individual data set is too small for a true refinement of the parameters (this must be done on the whole set of data). But there should not be, on the other hand, marked differences in the answers from each data set; if this were the case, we should come back to the experiment, look for errors in the program, or conclude that an important parameter is still lacking in the models being tested.

An important point concerns the relative intensities among beams. Generally, including the present work, each $I(V)$ spectrum is normalized independently so that the information on relative intensities is discarded. It can, however, be restored by calculating the ratio of the integrated experimental to theoretical intensities, $R_g=\sum_E I_{expt}(E)/\sum_E I_{theor}(E)$ for the g beam. Being light measurements, the experimental intensities are not normalized on an absolute scale, thus only the dispersion of the ratio R_g can be discussed. In the present study,

TABLE I. Optimum parameters and standard deviation for nitrogen atoms adsorbed in the fourfold hollow site (total data set). The bottom line gives the changes in the parameters corresponding to 1% increase of the metric distance from the minimum (see text).

	Metric min. (%)	d_{N1} (Å)	d_{12} (Å)	d_{23} (Å)	ΔV_R (eV)
D_1	11.65	0.21_7	1.79_1	1.39_1	−1.6
D_2	4.13	0.22_4	1.79_4	1.40_5	0.3
D_{2y}	2.46	0.21_9	1.79_7	1.40_3	−1.2
D_4	7.58	0.23_0	1.79_6	1.41_1	−1.2
D_{4y}	4.39	0.21_7	1.79_3	1.40_1	−1.4
Std. deviation		0.016	0.003	0.007	0.8
$\langle\ \rangle_{Di}$		0.22_1	1.79_4	1.40_2	−1.0
Δ_{param}		0.011	0.008	0.011	0.7

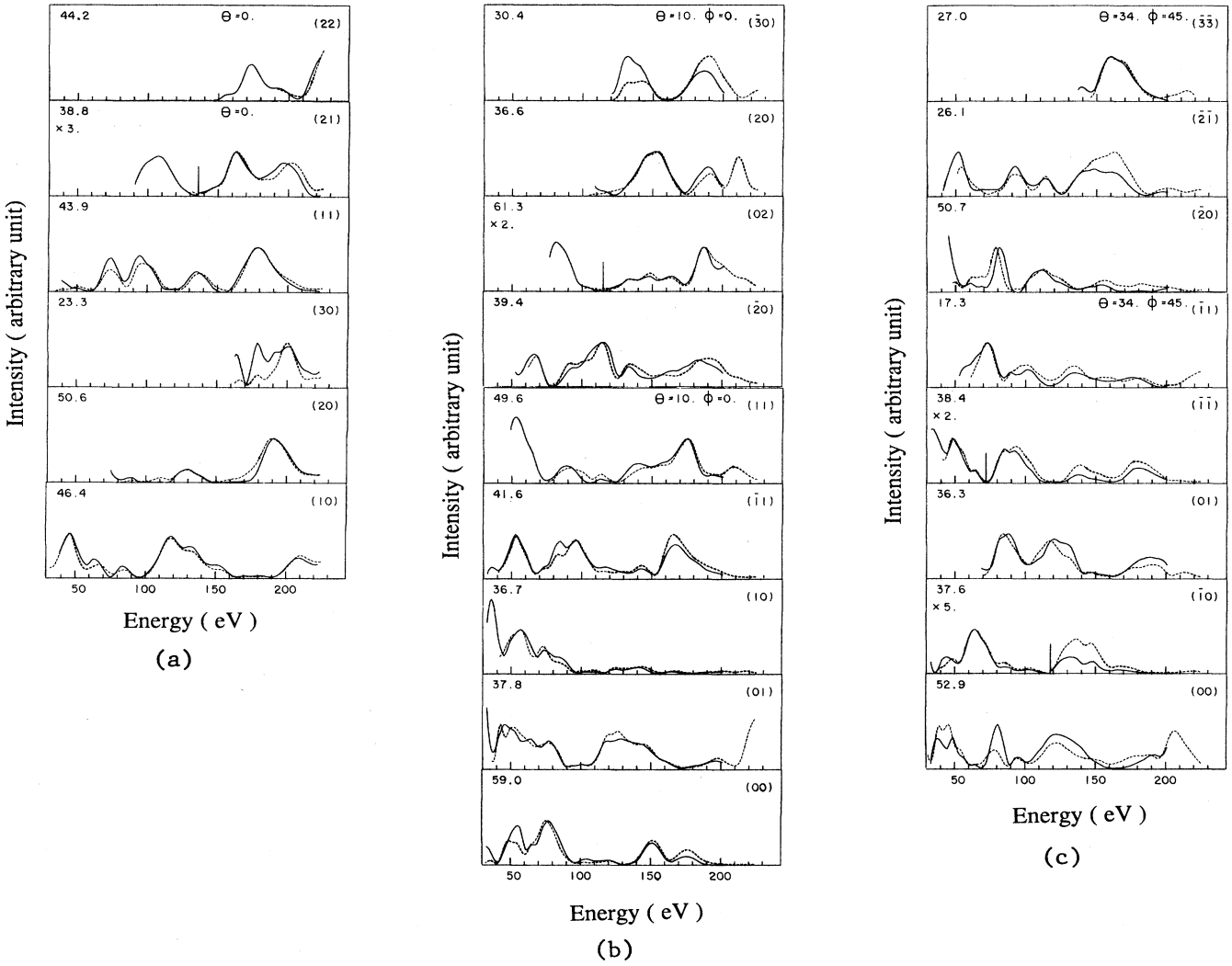

FIG. 5. Cr(100)-(1×1)N: $I(V)$ spectra for the best model. The numbers in the left corner denote the ratio R_g of the integrated experimental to theoretical intensities (see text): (a) normal incidence, (b) $(\theta,\phi)=(10°,0°)$, and (c) $(\theta,\phi)=(34°,45°)$.

the average value of R_g over the various $I(V)$ curves is 40 ± 10 (see Fig. 5), the worst deviations being 17 and 60. Most of the R_g are within a factor less than 2. The interesting fact is that *this dispersion reduces when the structural model approaches the optimum,* giving an extra argument in favor of the proposed model. This is similar to the $I(g)$ method introduced by Clarke[23] to extract the structure from LEED intensities. This method, which relies on the relative intensities only, proved successful and faster than the standard $I(V)$ analysis for Ni(110).[24]

2. *Accuracy of the parameters*

In order to develop an intuition for errors in the parameters, we can look at two complementary pieces of information.

TABLE II. Best structural parameters, averaged over the five metric distances, for the different beam sets.

(θ,ϕ)		d_{N1} (Å)	d_{12} (Å)	d_{23} (Å)	ΔV_R (eV)
(0°,0°)	$\langle\ \rangle_{Di}$	0.23_1	1.80_4	1.42_3	0.5
	Std. deviation	0.004	0.014	0.004	0.6
(10°,0°)	$\langle\ \rangle_{Di}$	0.23_4	1.79_8	1.39_2	−0.8
	Std. deviation	0.005	0.001	0.004	0.6
(34°,45°)	$\langle\ \rangle_{Di}$	0.17_9	1.77_8	1.40_5	−1.6
	Std. deviation	0.039	0.002	0.007	0.3

(i) The standard deviations from the answers of the five metrics on the whole data set (Table I) probably underestimate the total error. However, they increase the certainty that the correct model has been identified.

(ii) We can "measure" the change in each parameter near its optimum value when each metric distance is changed from its best value. Since, close to the optimum structure, the metric can be fitted by a hyperellipsoid against each parameter, a scale of the uncertainty can be given for each parameter by the deviation corresponding to a 1% change in the metric distance above the absolute minimum. This has been done for the whole data base and is summarized at the bottom of Table I.

To discuss these numbers we have several more facts to consider.

(i) 1% variation is arbitrary and *serves only as a scaling quantity.* This helps to deduce the actual uncertainty corresponding to any other (more realistic?) value for a significant deviation from the minimum of the metric distance: for instance, 4% deviation from the minimum metric distance, instead of 1%, would only yield a factor of 2 on the range of uncertainty of the parameters discussed above. This is only valid for small variations away from the minimum.

(ii) Another way to estimate the uncertainty obtained by LEED is to compare careful work published on the same surface. This is available for very few systems, but the case of Ni(110) is perhaps the most instructive. Three groups[15,25,26] have looked at this surface, totally independently, using different samples, different preparation techniques, different LEED setup and acquisition means, different LEED programs, and different criteria for the quantitative comparison between experimental and theoretical spectra. Their answers are the following: $d_{12}=(1.141$ Å, 1.137 Å, 1.140 Å), $d_{23}=(1.284$ Å, 1.283 Å, 1.289 Å), yielding the average answers and dispersions $d_{12}=1.139\pm0.002$ Å, $d_{23}=1.285\pm0.003$ Å.

From the above discussion it follows that the reproducibility from one work to another one is excellent. For the present study, the agreement between experiment and theory is better than for the Ni(110) case (the metric distance D_1 for instance is 11.6 instead of 12.9) which can be considered as a good reference. A good estimate of the final accuracy can be obtained in Table I from the maximum value between the standard deviation and the 1% uncertainty as defined above.

3. *Optimum structural model*

The self-consistency of the results increases the confidence in the model identified: Nitrogen is located in the fourfold hollow site (HO) at a distance $d_{N1}=0.221\pm0.016$ Å above the substrate, producing a "mixed buckled layer." The interlayer spacing oscillates around the bulk value and is strongly damped on two layers: $d_{12}=1.794\pm0.008$ Å (~24.8% expansion with respect to the bulk x-ray value, 1.4375 Å) and $d_{23}=1.402\pm0.011$ Å (−2.5% contraction).

The muffin-tin radius $R_{MT}(N)$ turns out to be weakly dependent on the other variables, i.e., changing its value does not influence measurably the optimum geometrical parameters, although it modifies slightly the structures of the $I(V)$ spectra. Optimizing R_{MT} improves the total metric distance by as much as 10% and helps in reducing the already small dispersion in the response of the metric distances. All metric distances show a clear minimum at $R_{MT}(N)=0.85$ Å. In a hard sphere model, assuming a chromium radius $R_{Cr}=1.245$ Å (bulk value), N ends with a radius $R_N=0.77$–0.80 Å, i.e., slightly less than the value from LEED optimization, $R_{MT}=0.85$ Å. Such overlaps are common with adsorbates as pointed out in different works on sulfur,[3] iodine,[27] and cesium[21] adsorbed at metal surfaces. In the present study, the radius increase might be interpreted qualitatively as the result of a charge transfer from the metal to nitrogen, as found for bulk nitrides[7] or carbides.[9]

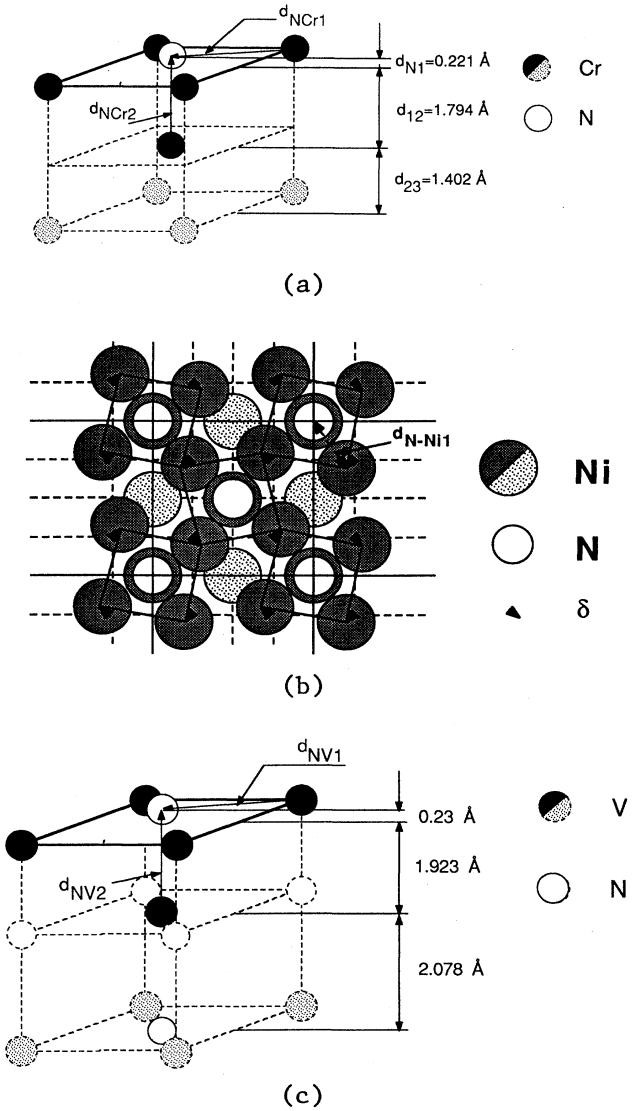

FIG. 6. Local environment of N atoms: (a) Cr(100)-(1×1)-N surface; (b) Ni(100)-*P4g*-N, top view: the unit mesh is a 2×2 superstructure made of squares (enlarged and rotated by the presence of N atoms at their center) and of rhombs to accommodate the strain; the parameter ∂ is a measure of the amount of distortion; and (c) $VN_{0.89}(100)$ surface.

IV. DISCUSSION

A. Local environment of surface nitrogen

The geometrical arrangement of the surface is illustrated in Fig. 6(a). Nitrogen atoms are bound to four surface chromium atoms at a distance $d_{NCr1}=2.045\pm0.002$ Å but also to a fifth Cr atom, located directly below the N in the second layer at $d_{NCr2}=2.015\pm0.018$ Å. Preferential bonding to metallic atoms in layer 2 was already noticed in the case of sulfur adsorbed on Ni(110).[3] In the present case, N resides in a five-neighbor coordination site, forcing the interlayer distance d_{12} to expand by as much as $24.8\pm0.6\%$. In that respect also, it is similar to S/Ni(110) in the sense that S adsorption causes a relaxation reversal of the interlayer distance d_{12} in Ni(110) which transforms from an 8.5% contraction at the clean surface to a 10% expansion upon sulfur chemisorption; at the same time the distances d_{SNi1} and d_{SNi2} become equal to 2.32 and 2.21 Å, respectively.

B. Comparison with other systems

N gives rise to a $c(2\times2)$ LEED pattern when adsorbed on Fe(100) ($\frac{1}{2}$ monolayer coverage)[28] instead of a (1×1) pattern as for Cr(100) (1 monolayer coverage). As far as iron is concerned, N atoms are also located in the hollow sites, but the distance $d_{NFe2}=1.83$ Å to the fifth metallic atom is much shorter than for Cr, the interlayer spacing d_{12} is expanded by 10% instead of 25% for Cr, while the interatomic distance $d_{NFe1}=2.04$ Å is exactly that found with chromium. Surface Fe atoms have fewer N neighbors since the coverage is only 0.5, so that the bond strength with the second layer atoms is increased resulting in a shortening of d_{12}. In that case the nitrogen hard sphere radius has now values from 0.6 to 0.8 Å.

Although less direct, a comparison can be made with N/Ni(100), which is a fcc metal. The accepted adsorption site, for half-monolayer coverage, as found by EXAFS, is the center of disorted and rotated squares at 0.1 Å above the substrate, and N is bound to five Ni atoms.[29] The N-Ni distances are 1.89 and 1.87 Å (vertical distance), i.e., noticeably shorter than for Cr [see Fig. 6(b)]. Unfortunately, the interlayer spacing d_{12} was assumed to be the bulk value, so that the vertical distance is questionable because an expansion of d_{12} is very likely in the light of many studies of adsorbates including this one [for instance S on Ni(110),[3] N on Fe(100) (Ref. 28)]. Nevertheless, nitrogen atoms induce a strong lateral distortion to reproduce a local environment equivalent to the one we conclude to be the case of N/Cr(100).

The similarity is even more striking with the surface of a bulk nitride, namely $VN_{0.89}(100)$.[30] As shown in Fig. 6(c), preliminary calculations show that the first mixed layer is buckled, with N atoms located at 0.23 Å above the vanadium sublayer (very close to 0.22 Å for Cr). In the meantime d_{12} contracts (-7%) until N atoms have in-plane vanadium neighbors at 2.15 Å, which happens to be 6.5% longer (2.15 instead of 2.02 Å) than for Cr. This, very likely, follows from the presence of bulk nitrogen atoms which increase the number of bonds and consequently lower the bond strengths between N surface atoms and vanadium atoms in layer 2.

V. CONCLUSION

We have presented a quantitative LEED analysis of the Cr(100)-(1×1)-N surface structure resulting from nitrogen chemisorption to form a surface nitride. Emphasis has been put on the local environment of N atoms, and a comparison has been made with other known surface structures, either of surface nitrides or of the surface of bulk nitrides.

The nitrogen atoms sit in the symmetric fourfold hollows very slightly above the top Cr layer ($d_{N1}=0.22$ Å). A very strong expansion (24.8%) of the metallic interlayer distance d_{12} occurs in such a way that the four Cr neighbors in the top layer and the fifth Cr atom in the second layer are at very similar distances (2.045 and 2.015 Å, respectively).

We have compared our results with other similar surfaces, Fe(100)-$c(2\times2)$-N, Ni(100)-$p(2\times2)$-N, and $VN_{0.89}(100)$. In all four instances, differing either by the chemical species or by the coverage or finally by their bulk structure (bcc, fcc, NaCl) the most favorable situation is as close as possible to a five-neighbor coordination site, allowed at the price, in some circumstances, of drastic vertical or in-plane relaxation of the underlying substrate.

The list is certainly not exhaustive and similar local environment can be expected for carbon and other bulk compounds. Photoemission and band-structure calculations should provide valuable information for the knowledge of these structures. In particular it is interesting to measure possible charge transfers which seem to be the rule for bulk nitrides and carbides [0.3e for TiC,[31] 1.2e for VN,[7] 2.1e for $TiC_{0.94}$,[7] and 1.9e for $TiN_{0.99}$ (Ref. 7)] and may appear in the form of the large muffin-tin radius found by LEED for N/Cr and N/Fe. A quite natural extension of this study is to look at the influence of the crystallographic orientation.

ACKNOWLEDGMENTS

We are indebted to L. J. Clarke and R. Riedinger for very helpful discussions in the preliminary stage of the analysis, and to W. Moritz for providing the FORTRAN code used for the calculations. The Laboratoire de Spectrométre Physique is "Unite associé au Centre National de la Recherche Scientifique."

[1] J. D. Dunitz, J. B. Goodenough, P. Hemmerich, J. A. Ibers, C. K. Jorgensen, J. B. Neilands, D. Reinen, and R. J. Williams, Struct. Bonding (Berlin) **38** (1979).

[2] J. M. MacLaren, J. B. Pendry, P. J. Rouss, D. K. Saldin, G. A. Somorjai, M. A. Van Hove, and D. D. Vvedensky, *Surface Crystallographic Information Service* (Reidel, Dordrecht, 1987).

[3] R. Baudoing, Y. Gauthier, and Y. Joly, J. Phys. C **18**, 4061 (1985).

[4] L. E. Toth, *Transition Metal Carbides and Nitrides* (Academic,

London, 1971).
[5]J. E. Sundgren and T. G. Hentzell, J. Vac. Sci. Technol. A **4**, 2259 (1986).
[6]A. Neckel, P. Rastl, R. Eibler, P. Weinberger, and P. K. Schwarz, J. Phys. C **9**, 579 (1976).
[7]F. Kubel, H. D. Flack, and K. Yvon, Phys. Rev. B **36**, 1415 (1987).
[8]P. A. Lindberg and L. I. Johansson, Surf. Sci. **194**, 199 (1988).
[9]E. Winner, A. Neckel, and A. J. Freeman, Phys. Rev. B **31**, 2370 (1985).
[10]L. de Bersuder, Rev. Sci. Instrum. **45**, 1569 (1974).
[11]W. Moritz (private communication).
[12]L. Hedin and B. I. Lundqvist, J. Phys. C **4**, 2064 (1971).
[13]S. A. Lindgren, L. Walldén, J. Rundgren, and P. Westrin, Phys. Rev. B **29**, 576 (1984).
[14]Y. Gauthier, R. Baudoing, and L. J. Clarke, J. Phys. C **15**, 3231 (1982).
[15]Y. Gauthier, R. Baudoing, Y. Joly, C. Gaubert, and J. Rundgren, J. Phys. C **17**, 4547 (1984).
[16]J. Philip and J. Rundgren, in *Determination of Surface Structure by LEED,* edited by P. M. Marcus and F. Jona (Plenum, New York, 1984).
[17]Y. Gauthier, R. Baudoing, Y. Joly, and J. Rundgren, Phys. Rev. B **31**, 6216 (1985).
[18]R. Baudoing, Y. Gauthier, M. Lundberg, and J. Rundgren, J. Phys. C **19**, 2825 (1986).
[19]Y. Gauthier, R. Baudoing, M. Lundberg, and J. Rundgren, Phys. Rev. B **35**, 7867 (1987).
[20]Y. Gauthier, R. Baudoing, and J. Jupille, Phys. Rev. B **40**, 1500 (1989).
[21]S. A. Lindgren, L. Walldén, J. Rundgren, P. Westrin, and J. Neve, Phys. Rev. B **28**, 6707 (1983).
[22]H. D. Shih, F. Jona, D. W. Jepsen, and P. M. Marcus, Phys. Rev. Lett. **36**, 798 (1975).
[23]L. J. Clarke, Vacuum **29**, 405 (1979).
[24]L. J. Clarke, R. Baudoing, and Y. Gauthier, J. Phys. C **15**, 3249 (1982).
[25]D. L. Adams, L. E. Petersen, and C. S. Sorensen, J. Phys. C **18**, 1753 (1985).
[26]W. Reimer, V. Penka, M. Skottke, R. J. Behm, G. Ertl, and W. Moritz, Surf. Sci. **186**, 45 (1987).
[27]M. Maglietta, E. Zanazzi, U. Bardi, D. Sondericker, F. Jona, and P. M. Marcus, Surf. Sci. **123**, 141 (1982).
[28]R. Imbilhl, R. J. Behm, G. Ertl, and W. Moritz, Surf. Sci. **123**, 129 (1982).
[29]L. Wenzel, D.Arvanitis, W. Doum, H. Rotermundh, J. Stöhr, K. Baberschke, and H. Ibach, Phys. Rev. B **36**, 7689 (1987).
[30]Y. Gauthier, Y. Joly, J. Rundgren, P. Wincott, and L. I. Johansson (unpublished).
[31]E. Wimmer, A. Neckel, and A. J. Freeman, Phys. Rev. B **31**, 2370 (1985).